A Nested Array Geometry with Enhanced Degrees of Freedom and Hole-Free Difference Coarray

Steven Wandale and Koichi Ichige
Department of Electrical and Computer Engineering, Yokohama National University
79-5 Tokiwadai, Hodogaya-ku, Yokohama, Kanagawa 240-8501, Japan.

***Abstract*—This paper presents a new extended nested array geometry with enhanced degrees-of-freedom (DOFs) and a hole-free difference coarray for Direction-of-Arrival (DOA) estimation applications. The array is developed by distributing the sensor of the dense section of the nested array to the nested array's outer subarray while retaining a hole-free difference coarray. The rendered extended nested array has enhanced array aperture and a hole-free difference coarray compared to most existing nested array configurations. Moreover, the proposed array has a closed-form expression for array sensor location and reduced mutual coupling due to sparsely located sensors. Numerical simulations show that the proposed array offers improved DOA estimation resolution than other conventional sparse arrays due to the enhanced aperture.**

***Index Terms*—Nested array, sparse arrays, direction-of-arrival estimation, extended aperture, difference coarray.**

I. Introduction

Direction-of-Arrival (DOA) estimation is one of the useful techniques in the array signal processing field for detection and localization of array input signals [1]–[2]. Hence, it has a wide range of applications in sonar, automotive radar, imaging, and wireless communication systems [3]. Conventionally, uniform linear arrays (ULAs) are commonly used, where the sensors are placed at a half-wavelength from each other to avoid spatial aliasing. However, ULAs have limited degrees of freedom (DOFs) such that given M sensors, ULA can resolve up to $M-1$ sources. Moreover, they suffer from the mutual coupling between sensors owing to the closely spaced sensors [5].

To circumvent the above issues, non-uniform arrays (also known as sparse arrays) have become more attractive than conventional ULAs for several reasons. Firstly, in the view of the difference coarray (DCA) concept, sparse arrays can achieve enhanced DOFs and resolve more uncorrelated sources than the number of sensors [5]. Secondly, the larger interelement spacing between sparse arrays sensors enables them to reduce the mutual coupling effect between sensors compared to their conventional ULA counterparts [3]–[6].

The common prototype sparse arrays include minimum redundancy arrays (MRAs) [3], minimum hole arrays (MHAs) [4], coprime arrays (CAs) [5] and nested linear arrays (NAs) [6]. However, despite having some of the properties of sparse arrays, these sparse arrays have limitations. The MRAs and MHAs lack closed-form expressions for sensor location [5]–[6]. Also, coprime arrays have holes in their DCA. Hence, the realized DOFs are lower than in MRAs, and NAs [6]. Furthermore, NAs exhibit severe mutual coupling effect due to the existence of a dense uniformly spaced subarray [7].

Recently, motivated by limitations of the prototype sparse arrays, i.e., NAs and CAs, several modifications aiming to enhance the DOFs and reduce mutual coupling effect have been proposed [8]. Some of NA's and CA's variants that have been proposed include super nested array (SNA) [7], generalized nested array (GNA) [9], generalized coprime array (GCA) [10], thinned coprime array (TCA) [11], augmented nested array (ANA) [12], enhanced nested array (ENA) [13], improved nested array (INA) [14], Iizuka NA [15], sparse array with maximum interelement spacing constraint (MISC) [16] and one-side extended nested array (OS-ENA) [17]. Nonetheless, some variant arrays, such as SNA, share the same DOFs or less with the parent arrays. Additionally, INA and ENA still retains the prototype NA's dense subarray and suffer severe mutual coupling effects. Moreover, the DCA of sparse arrays such as GCA, GNA, and TCPA, are not hole-free. As a result, they have small DOFs compared to their parent arrays.

This paper proposes an enhanced nested array with multiple subarrays (ENAMS) with enhanced DOFs and reduced mutual coupling. The ENAMS array is designed by splitting the nested array into several sparse subarrays with different sensor separations. The sparse sensor separation enables ENAMS to possess enhanced DOFs and reduced mutual coupling compared to NA, ENA, and INA with the same number of sensors. More importantly, the ENAMS array enjoys all the nested array's desired properties, such as hole-free difference coarray and closed-form expression, to determine sensor locations. Numerical simulations and theoretical analysis are used to demonstrate the superiority of the proposed sparse array. The results show that the proposed array has superior DOA estimation performance than other conventional sparse arrays through simulations.

$Notations$: Throughout the paper, we use lower-case and upper-case bold characters to denote vectors and matrices, respectively, i.e., $\boldsymbol{I}_K$ represents the $K \times K$ identity matrix. Operators $(\cdot)^T$ and $(\cdot)^H$ stand for transpose and the conjugate transpose of a vector or matrix in that order. And, vec$(\cdot)$ denotes vectorization operator and diag$(\cdot)$ represents a diagonal matrix. Moreover, $\otimes$ and $E\left[\,\cdot\,\right]$ denote the Kronecker product and statistical expectation operator respectively.

This work was supported in part by Japan Society for the Promotion of Science (JSPS) Grant-in-Aid for Scientific Research no. 20K04500. The authors are sincerely grateful for their support.

II. Preliminaries

A. Array Signal Model

Assume that K uncorrelated narrowband sources from far field directions $\theta_1, \theta_2, ..., \theta_k$, for $k = 1, 2, ..., K$ impinge on a $M-$element sparse linear array. Then, in the presence of mutual coupling the received signal vector $\boldsymbol{x}(t) = [x_1(t), x_2(t), \cdots, x_M(t)]^T$ at $t-$th snapshot can be expressed as

$$\boldsymbol{x}(t) = \boldsymbol{C}\boldsymbol{A}(\theta)\boldsymbol{s}(t) + \boldsymbol{n}(t), \tag{1}$$

where $\boldsymbol{s}(t) = [s_1(t), s_2(t), \cdots, s_K(t)]^T$ and $\boldsymbol{n}(t)$ are the source signal and the noise vector respectively. And, $\boldsymbol{A} = [\boldsymbol{a}(\theta_1), \boldsymbol{a}(\theta_2), \ldots, \boldsymbol{a}(\theta_K)]$ is the array manifold whose k-th source steering vector $a(\theta_k)$ can be expressed as

$$\boldsymbol{a}(\theta_k) = [1, e^{jd_2\kappa\sin(\theta_k)}, \ldots, e^{jd_M\kappa\sin(\theta_k)}]^T, \tag{2}$$

where $\kappa = 2\pi/\lambda$, and λ is the carrier's frequency wavelength. The matrix $\boldsymbol{C}$ is mutual coupling matrix which can be approximated by a B-banded mode [7]

$$\boldsymbol{C} = \begin{cases} c_{|d_1-d_2|}, & |d_1 - d_2| \leq B \\ 0, & |d_1 - d_2| > B \end{cases} \tag{3}$$

which satisfies $1 = c_0 > |c_1| > |c_2| > \cdots > |c_B|$. Thus, assuming that the signals and the noise are uncorrelated spatially and temporally, the covariance matrix of (1) can be expressed as

$$\boldsymbol{R}_x = E\big[\boldsymbol{x}(t)\boldsymbol{x}^H(t)\big] = \boldsymbol{C}\boldsymbol{A}\boldsymbol{R}_s\boldsymbol{A}^H\boldsymbol{C}^H + \sigma_n^2\boldsymbol{I}_M, \tag{4}$$

where $\boldsymbol{R}_s = \mathrm{diag}([\rho_1^2, \rho_2^2, \ldots, \rho_K^2])$ with ρ_k^2 and σ_n^2 being signal and noise powers respectively [16]. In practical, the sampled snapshots are limited as such (4) can be approximated as

$$\tilde{\boldsymbol{R}}_x = \frac{1}{T}\sum_{t=1}^{T}\boldsymbol{x}(t)\boldsymbol{x}^H(t). \tag{5}$$

B. Difference Co-array

Following [6] –[16], vectorizing (4) yields

$$\boldsymbol{y} = \mathrm{vec}(\boldsymbol{R}_x) = \tilde{\boldsymbol{C}}\tilde{\boldsymbol{A}}\boldsymbol{Q} + \sigma_n^2\mathcal{I}, \tag{6}$$

where $\tilde{\boldsymbol{C}} = (\boldsymbol{C}^* \otimes \boldsymbol{C})$, $\tilde{\boldsymbol{A}} = [\tilde{\boldsymbol{a}}(\theta_1), \tilde{\boldsymbol{a}}(\theta_2), \ldots, \tilde{\boldsymbol{a}}(\theta_K)]$ is the extended virtual array manifold with $\tilde{\boldsymbol{a}}(\theta_k) = (\boldsymbol{a}(\theta_k)^* \otimes \boldsymbol{a}(\theta_k))$ denoting the virtual steering vector. In other words, $\tilde{\boldsymbol{A}}$ can be regarded as a difference coarray. Additionally, $\boldsymbol{Q}$ represents the equavalent signal vector, $\boldsymbol{y}$ becomes the new received signal vector and $\mathcal{I} = \mathrm{vec}(\boldsymbol{I}_M)$.

Definition 1. *(Difference Coarray): Given a sparse array $\mathbb{Z}_p$, the difference coarray [7] of $\mathbb{Z}_p$ is defined as*

$$\mathbb{D}_p = \{d_1 - d_2 | d_1, d_2 \in \mathbb{Z}_p\}. \tag{7}$$

Definition 2. *(Uniform DOF): Given a sparse array $\mathbb{Z}_p$, the number of elements in the consecutive segment of its difference coarray $\mathbb{D}_p$ is known as "Uniform DOF," i.e., $uDOF$ [14].*

This implies that the number of uncorrelated sources that any subspace method i.e., coarray MUSIC [18], can resolve is up to $(uDOF - 1)/2$ [17].

Definition 3. *(Weight Function): The weight function $w(m)$ of a sparse array $\mathbb{Z}_p$ is the pair of sensors that contributes to coarray index m [7], i.e.,*

$$w(m) = |\{(d_1, d_2) \in \mathbb{Z}^2 | d_1 - d_2 = m\}|, m \in \mathbb{D}_p. \tag{8}$$

In the subsequent sections, we will use the definitions above to evaluate the qualities of the proposed array.

III. Extended nested array with multiple subarrays

This section presents an extended nested array with multiple subarrays and its main properties considering the maximum achievable DOFs and mutual coupling effect. The comparisons between ENAMS and other existing sparse arrays are also given.

Definition 4. *For a pair of integers $M_1 \geq 4$ and $M_2 \geq 2$, the configuration of the ENAMS array can be defined as*

$$\mathbb{Z}_p = \mathbb{Z}_1 \cup \mathbb{Z}_2 \cup \mathbb{Z}_3 \cup \mathbb{Z}_4 \cup \mathbb{Z}_5 \tag{9}$$

where

$$\begin{aligned}
&\mathbb{Z}_1 = \{1 + (\ell_1 - 1) | \ell_1 = 1, 2, \cdots, M_1 - 2\}, \\
&\mathbb{Z}_2 = M_1 + 1, \\
&\mathbb{Z}_3 = \{2M_1 + \ell_2(M_1 + 1) | \ell_2 = 0, 1, \cdots, M_2 - 2\}, \\
&\mathbb{Z}_4 = M_2(M_1 + 1), \\
&\mathbb{Z}_5 = M_2(M_1 + 1) + M_1 - 2.
\end{aligned}$$

To appreciate the construction of the proposed array, let us consider a nested array shown in Fig. 1 (a). The nested array consists of two connected ULAs with different interelement spacing. The first ULA consists of M_1 elements with a unit interelement spacing $\lambda/2$ and the second ULA comprises of M_2 elements with the interelement spacing of $(M_1 + 1)\lambda/2$ [6]. For simplicity, henceforth we normalize $\lambda/2$ to 1.

Based on the structure of nested array, the proposed array is characterized by (9) where subarrays $\mathbb{Z}_1$, $\mathbb{Z}_2$, and $\mathbb{Z}_4$ are constructed by splitting the dense-ULA of nested array whereas subarrays $\mathbb{Z}_3$ and $\mathbb{Z}_5$ are developed from the sparse-ULA of NA. In particular, $\mathbb{Z}_1$ consists of $(M_1 - 2)$ sensors with a unit spacing, $\mathbb{Z}_2$ and $\mathbb{Z}_4$ each contains a single sensor at locations $(M_1 + 1)$ and $M_2(M_1 + 1)$ respectively. For the remaining sets, $\mathbb{Z}_3$ comprises of $(M_2 - 1)$ sensors placed at a spacing of M_1 from each other and the remaining sensor of M_2 is placed at $M_2(M_1 + 1) + M_1 - 2$ as set $\mathbb{Z}_5$.

In order to verify the validity of (9), let us consider a formulation using $M_1 = 4$ and $M_2 = 6$. Then, the definition in (9) renders $\mathbb{Z}_1 = \{1, 2\}$, $\mathbb{Z}_2 = \{5\}$, $\mathbb{Z}_3 = \{8, 13, 18, 22, 28\}$, $\mathbb{Z}_4 = \{30\}$ and $\mathbb{Z}_5 = \{32\}$ thereby yielding a sparse array as shown in Fig. 1 (b).

The proposed ENAMS array defined in (9) has the following properties:

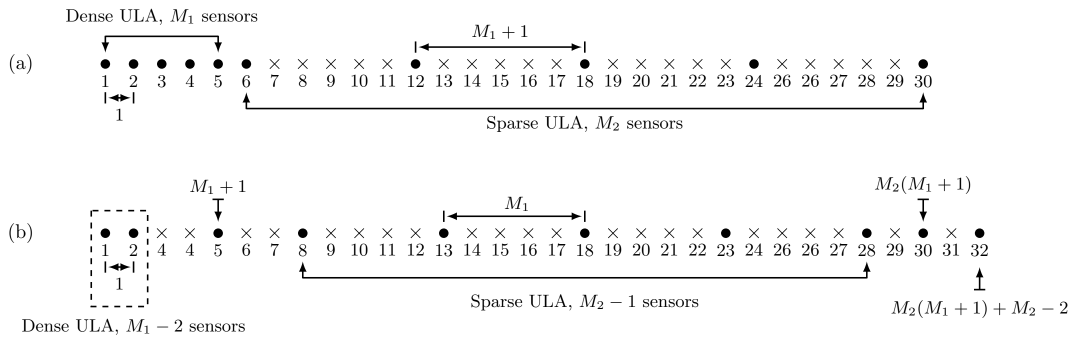

Fig. 1: Sparse array configuration of (a) nested array with $M_1 = M_2 = 5$ and (b) proposed ENAMS array with $M_1 = 4$ and $M_2 = 6$. The bullets and crosses denote physical sensors and empty spaces respectively.

TABLE I: Optimal Solution for ENAMS Configuration

M	Optimal, M_1, M_2	Maximum $uDOF$
Even	$M_1 = M_2 = M/2$	$M^2/2 + 2M - 1$
Odd	$M_1 = (M-1)/2$ $M_2 = (M+1)/2$	$M^2/2 + 2M - 4.5$

Proposition 1. *For $M_1 \geq 4$ and $M_2 \geq 2$, the DCA of the proposed array is hole-free.*

Proof. The proof of Proposition 1 is shown in Appendix A. □

Proposition 2. *For a given number $M = M_1 + M_2$, the ENAMS array achieves maximum $uDOF$ of $M^2/2 + 2M - 1$.*

Proof. As described in Proposition 1, the DCA of the ENAMS array is hole-free and ranges from $-(M_2(M_1+1)+M_2-3)$ to $M_2(M_1+1)+M_2-3$, i.e.,

$$\begin{aligned}\mathbb{D}_p = \{&-(M_2(M_1+1)+M_2-3), \ldots, \\ &-2, -1, 0, 1, 2, \ldots, M_2(M_1+1)+M_2-3\}.\end{aligned} \quad (10)$$

Since, DCA is symmetric about zero, the one-side consecutive DOFs are $d_u = M_2(M_1+1)+M_2-3$. Then, the whole consecutive DOFs are $\mathcal{D} = 2d_u+1 = 2M_2(M_1+1)+2M_2-5$. As such, maximum DOFs under the constraint of number of $M = M_1 + M_2$ can be cast as the following optimization problem:

$$\begin{aligned}\max_{M_1, M_2} \quad & \mathcal{D} = 2M_2(M_1+1)+2M_2-5 \\ \text{subject to} \quad & M = M_1 + M_2\end{aligned} \quad (11)$$

Problem (11) can be solved using arithmetic mean-geometric mean inequalities, and the solution is summarized in Table I. □

Remark: Thus, for optimal number of M_1 and M_2 the proposed array has four more DOFs than nested and super nested array. However, the opposite is true in a case of ENAMS and minimum redanducy array.

Considering weight functions, the first three functions– $w(1)$, $w(2)$ and $w(3)$, contribute considerably to mutual coupling effects. Hence, the robustness of a sparse array to mutual coupling can be judged based on these weight functions' values. The smaller the values of the three weight functions, the lower the mutual coupling effect and vice versa [8]. And, for $M_1 \geq 4$ and $M_2 \geq 2$ the proposed array satisfies the following weight functions

$$w(1) = M_1 - 3, \quad w(2) = 3 \quad \text{and} \quad w(3) = 2. \quad (12)$$

In contrast, the first three weight functions of the nested array are

$$w(1) = M_1, \quad w(2) = M_1 - 1 \quad \text{and} \quad w(3) = M_1 - 2. \quad (13)$$

and those of super nested array include

$$w(1) = \begin{cases} 1, & \text{if } M_1 \text{ is even} \\ 2, & \text{if } M_1 \text{ is odd} \end{cases} \quad (14)$$

$$w(2) = \begin{cases} M_1 - 3, & \text{if } M_1 \text{ is even} \\ M_1 - 1, & \text{if } M_1 \text{ is odd} \end{cases} \quad (15)$$

$$w(3) = \begin{cases} 3, & \text{if } M_1 = 4, 6, \\ 4, & \text{if } M_1 \text{ is even } (M_1 \geq 8), \\ 1, & \text{if } M_1 \text{ is odd.} \end{cases} \quad (16)$$

Comparing the weight function values of the ENAMS array with those of nested arrays and super nested arrays, the proposed array has reduced weights than nested arrays and comparable to those of super nested arrays as demonstrated in (12)–(16).

IV. Numerical Examples

In this section, we conduct simulations to compare the proposed array's performance with that of the nested array, super nested array, and minimum redundancy array (benchmark). For the nested array and the super nested array, we set $M_1 = 4$ and $M_2 = 6$ and $M_1 = 5$ and $M_2 = 5$ respectively. Furthermore, for the minimum redundancy array, we set $M = 10$. The sensor location of the super nested array ($\mathbb{Z}_{sna}$) and minimum

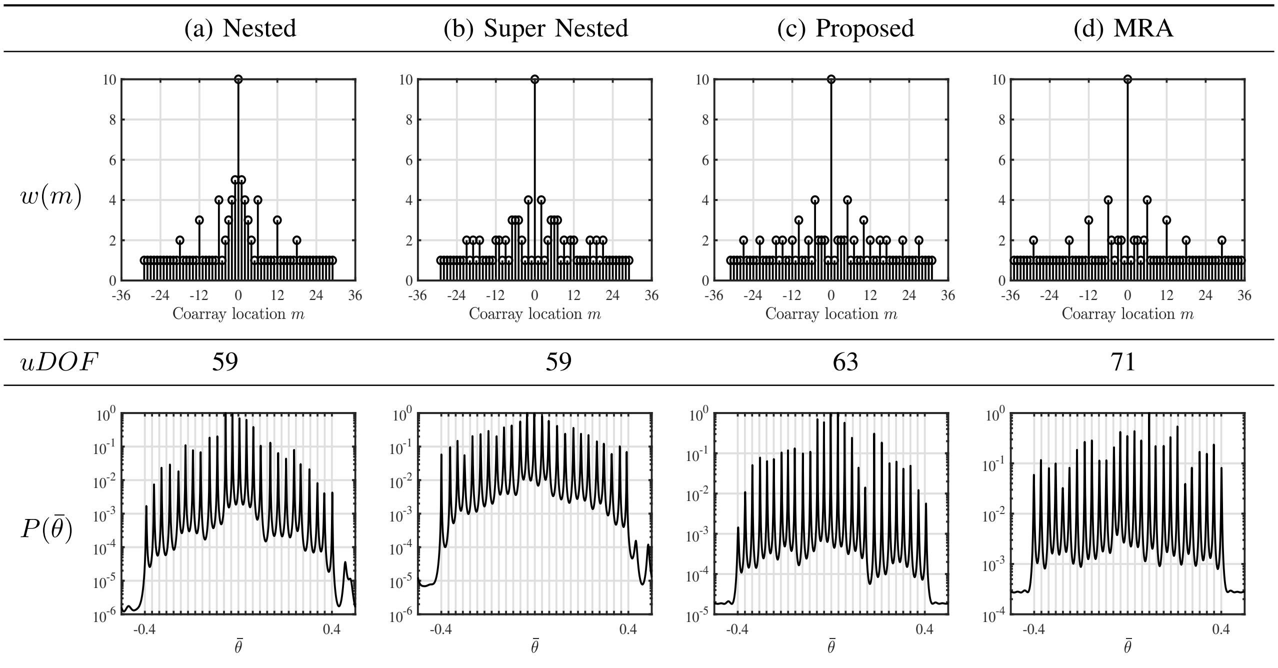

Fig. 2: Weight functions and MUSIC spectra $P(\bar{\theta})$ comparison among (a) nested arrays, (b) super nested arrays, (c) proposed array and (c) MRA in the presence of mutual coupling. The spectra is computed under $M = 10$, SNR = 0 dB, 500 snapshots and $K = 27$ sources marked by ticks on the $\bar{\theta}$ axis.

redundancy array ($\mathbb{Z}_{mra}$) are listed below (except for those of nested array and ENAMS which are shown in Fig. 1(a) and (b) respectively).

$$\begin{aligned} &\mathbb{Z}_{sna} = [1, 3, 5, 8, 12, 18, 24, 29, 30], \\ &\mathbb{Z}_{mra} = [1, 2, 5, 11, 17, 23, 29, 31, 34, 36]. \end{aligned} \tag{17}$$

In the first example, we evaluate the proposed array properties in comparison to other sparse arrays. The weight functions associated with various array configurations are shown in the first row of Fig. 2. It can be observed that all the arrays exhibit no holes in their DCAs, and the proposed array has four more DOFs than the nested and super nested array. The results are in line with propositions 1 and 2. Hence, the proposed array can resolve more sources than the nested and super nested arrays. Moreover, weight functions $w(1)$ of nested, super nested array, MRA, and the proposed array are 4, 1, 1, and 1 in that order. Hence, the proposed array shares reduced mutual coupling property with super nested array and MRA.

In the second example, we compare the MUSIC spectra $P(\bar{\theta})$ of DOA estimation of various array configurations as shown in the second row of Fig. 2. In this example, we assume 0 dB SNR, 500 Snapshots and $K = 27$ uncorrelated sources, located at $\bar{\theta}_k = -0.2 + 0.5(k-1)/26$ for $k = 1, 2, \cdots, 27$. Furthermore, we assume the signal model in (6) with the following mutual coupling parameters: $c_1 = 0.3e^{j\pi/3}$, $B = 100$ and $c_l = c_1 e^{j\pi(l-1)/8}/l$ for $1 \leq l \leq B$. It can be observed that only the MRA and proposed array resolved all sources correctly whereas the nested and super nested array show false peaks. The bahavior of super nested array in this case can be attributed to limited DOFs.

In the third and last example, we evaluate the performance of the arrays quantitatively using root-mean-square-error (RMSE) of DOA estimation, which can be defined as an average over η of trials:

$$RMSE = \sqrt{\frac{1}{\eta K} \sum_{i=1}^{\eta} \sum_{k=1}^{K} (\tilde{\bar{\theta}}_k^i - \bar{\theta}_k)^2}, \tag{18}$$

where $\tilde{\bar{\theta}}_k^i$ denotes $i-$th estimated normalized DOA for $i-$th trial and $\bar{\theta}_k$ is the true normalized DOA. Figure 3 illustrates the RMSE performance as a function of SNR and number of snapshots where 1000 trials are used. It can be observed that the performance of ENAMS improves with both SNR and number of snapshots compared to other sparse arrays except for MRA. The MRA outperform all arrays due to large aperture and sparserness. Nonetheless, the proposed array has improved performance compared to nested and super nested array due to enhanced DOFs.

V. Conclusion

This paper presented a new extended nested array geometry with multiple subarrays that provides enhanced DOFs and a hole-free difference coarray. The proposed array is designed to further distribute sensors within the outer subarray of a conventional nested array. The realized sparse array provides high-resolution DOA estimation compared to the conventional nested array and other well-known sparse arrays.

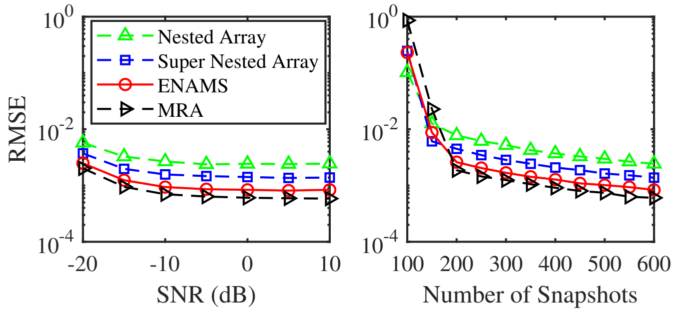

Fig. 3: Comparison of RMSE of DOA estimation among nested arrays, super nested arrays, proposed array and MRA in the presence of mutual coupling. The RMSE is computed under (left) $-20 \sim 10$ dB SNR with 500 snapshots and (right) $100 \sim 600$ snapshots with 0 dB SNR.

Appendix A: Proof of Proposition 1

Based on (10), a lag d satisfies $-M_2(M_1+)-M_2+3 \leq p \leq M_2(M_1+)+M_2-3$ for $M_1 \geq 4$ and $M_2 \geq 2$. Moreover, due to symmetric structure of the DCA, the following statements hold:

i) If d belongs in the coarray, then its mirror, i.e., $-d$ is also in the same coarray.

ii) The first sensor or self-difference of any one of the physical sensors contributes to lag $d = 0$.

As a result, it suffices to evaluate the scenario that $1 \leq d \leq M_2(M_1+) + M_2 - 3$. To that end, we consider the following cases.

a) If $1 \leq d \leq M_1 + 1$, d can be expressed as a difference between set $\mathbb{Z}_2$ and $\mathbb{Z}_1$, i.e., $\alpha_1 = \text{diff}(\mathbb{Z}_2, \mathbb{Z}_1)$. Namely,

$$\begin{aligned} \alpha_1 &= \{(M_1+1)\} - \{0, 1, \ldots, M_1 - 3\}, \\ &= \{0, 1, 2, \cdots, M_1, M_1 + 1\}. \end{aligned} \tag{19}$$

b) If $M_1 + 1 \leq d \leq 2M_1 + q(M_1 + 1)$ where $q = 0, 1, \ldots, M_2 - 2$, we can check first on $\alpha_2 = \text{diff}((2M_1 + q(M_1 + 1), \mathbb{Z}_1)$

$$\begin{aligned} \alpha_2 &= \{2M_1 + q(M_1+1)\} - \{0, 1, \ldots, M_1 - 2\} \\ &= \Big[\Big(\{2M_1\} - \{0, 1, \ldots, M_1 - 2\}\Big), \ldots, \\ &\quad \Big(\{2M_1 + q(M_1+1)\} - \{0, \ldots, M_1 - 2\}\Big)\Big]. \end{aligned} \tag{20}$$

Thus, (20) accounts for all lags between $M_1 + 1 \leq d \leq 2M_1 + q(M_1 + 1)$ and the rest of the lags can be easily filled by $\text{diff}(\mathbb{Z}_3, \mathbb{Z}_2)$, $(\mathbb{Z}_4, \mathbb{Z}_3)$, $(\mathbb{Z}_5, \mathbb{Z}_3)$, $(\mathbb{Z}_4, \mathbb{Z}_2)$ and $(\mathbb{Z}_5, \mathbb{Z}_2)$.

c) If $2M_1 + (M - 2)(M_1 + 1) \leq d \leq M_2(M_1 + 1)$, we can consider set $\alpha_3 = \text{diff}(\mathbb{Z}_4, \mathbb{Z}_1)$ which is equivalent to

$$\begin{aligned} \alpha_3 &= \{M_2(M_1+1)\} - \{0, 1, \ldots, M_1 - 3\}, \\ &= \{M_2(M_1+1) - (M_1 - 3), \cdots, \\ &\qquad M_2(M_1+1) - 1, M_2(M_1+1)\}. \end{aligned} \tag{21}$$

d) If $M_2(M_1 + 1) \leq d \leq M_2(M_1 + 1) + M_1 - 3$, we can check on a difference set between $\mathbb{Z}_5$ and $\mathbb{Z}_1$, i.e., $\alpha_4 = \text{diff}(\mathbb{Z}_5, \mathbb{Z}_1)$ which is equivalent to

$$\begin{aligned} \alpha_4 &= \{M_2(M_1+1) + M_1 - 3\} - \{0, 1, \ldots, M_1 - 3\}, \\ &= \{M_2(M_1+1), M_2(M_1+1) + (M_1 - 2), \cdots, \\ &\qquad M_2(M_1+1) + M_1 - 3\}. \end{aligned} \tag{22}$$

In general, the union of all the sets (19)-(22) and its counterpart set cover the consecutive integers from $-(M_2(M_1+1) - M_2 + 3)$ to $M_2(M_1+1) + M_2 - 3$, i.e., the DCA is hole-free.

References

[1] T. E. Tuncer and B. Friedlander, "Classical and modern direction of arrival estimation," *Academic Press*, 2009.

[2] P. Chevalier, L. Albera, A. Ferrool, P. Comon, "On the virtual array concept for higher order array processing," *IEEE Trans. Signal Processing*, vol. 53, no.4, pp. 1254-1271, Sep. 2005.

[3] A. Moffet, "Minimum-redundancy linear arrays," *IEEE Trans. Antennas Propagation*, vol. 16, no. 2, pp. 172-175, Mar. 1968.

[4] E. Vertatschitsch and S. Haykin, "Non-redundancy arrays," *Proc. in IEEE*, vol. 74, no.1, pp. 217-217, Jan. 1986.

[5] P. P. Vaidyanathan and P. Pal, "Sparse sensing with co-prime samplers and arrays," *IEEE Trans. Signal Processing*, vol. 59, no. 2, pp. 573-586, Feb. 2011.

[6] P. Pal and P. P. Vaidyanathan, "Nested arrays: A novel approach to array processing with enhanced degrees of freedom," *IEEE Trans. Signal Processing*, vol. 58, no. 8, pp. 4167-4181, Aug. 2010.

[7] C. Liu and P. P. Vaidyanathan, "Super nested arrays: Linear sparse arrays with reduced mutual coupling-Part I: Fundamentals," *IEEE Trans. Signal Processing*, vol. 64, no. 15, pp.3997-4014, Aug. 2016.

[8] S. Nakamura, S. Iwazaki and K. Ichige, "Optimization and Hole Interpolation of 2-D Sparse Arrays for Accurate Direction-of-Arrival Estimation," *IEICE Trans. Communications*, vol. E104-B, no. 4, pp. 401-409, Apr. 2021.

[9] J. Shi, G. Hu, X. Zhang and H. Zhou,"Generalized Nested Array: Optimization for Degrees of Freedom and Mutual Coupling," *IEEE Communications Letters*, vol. 22, no. 6, pp. 1208-1211, Jun. 2018.

[10] S. Qin, Y. D. Zhang and M. G. Amin, "Generalized Coprime Array Configurations for Direction-of-Arrival Estimation," *IEEE Transactions on Signal Processing*, vol. 63, no. 6, pp. 1377-1390, Mar. 2015.

[11] A. Raza, W. Liu and Q. Shen, "Thinned coprime arrays for DOA estimation," *Proc. of 2017 25th European Signal Processing Conference (EUSIPCO)*, pp. 395-399, 2017.

[12] J. Liu, Y. Zhang, Y. Lu, S. Ren and S. Cao, "Augmented nested arrays with enhanced DOF and reduced mutual coupling," *IEEE Transactions on Signal Processing*, vol. 65, no. 21, pp. 5549-5563, Nov. 2017.

[13] P. Zhao, G. Hu, Z. Qu and L. Wang, "Enhanced Nested Array Configuration With Hole-Free Co-Array and Increasing Degrees of Freedom for DOA Estimation," *IEEE Communications Letters*, vol. 23, no. 12, pp. 2224-2228, Dec. 2019.

[14] M. Yang, L. Sun, X. Yuan and B. Chen, "Improved nested array with hole-free DCA and more degrees of freedom," *Electronics Letters*, vol. 52, no. 25, p. 2068 – 2070, Dec. 2016.

[15] Z. Zheng, W. Wang, Y. Kong and Y. D. Zhang, "MISC Array: A New Sparse Array Design Achieving Increased Degrees of Freedom and Reduced Mutual Coupling Effect," *IEEE Transactions on Signal Processing*, vol. 67, no. 7, pp. 1728-1741, Apr. 2019

[16] Y. Iizuka and K. Ichige, "Extension of Nested Array for Large Aperture and High Degree of Freedom," *IEICE Communication Express*, vol. 6, no. 6, pp. 381-386, Jun. 2017.

[17] S. Ren, W. Dong, X. Li, W. Wang and X. Li, "Extended Nested Arrays for Consecutive Virtual Aperture Enhancement," *IEEE Signal Processing Letters*, vol. 27, pp. 575-579, 2020.

[18] C. Liu and P. P. Vaidyanathan, "Remarks on the Spatial Smoothing Step in Coarray MUSIC," *IEEE Signal Processing Letters*, vol. 22, no. 9, pp. 1438-1442, Sept. 2015.